A New Polythiophene Derivative for High Efficiency Polymer Solar Cells with PCE over 9%

Qunping Fan, Wenyan Su, Xia Guo, Bing Guo, Wanbin Li, Youdi Zhang, Kun Wang, Maojie Zhang,* and Yongfang Li**

As a promising next generation energy source technology, the bulk heterojunction (BHJ) polymer solar cells (PSCs) based on conjugated polymers as donor and fullerene derivatives as acceptor have attracted much interest due to their advantages such as low cost, light weight, and great potential of mass production of large area and flexible solar cell panels.[1–6] The key factors that determine the power conversion efficiency (PCE) of the PSCs are the open-circuit voltage (V_{oc}), short-circuit current density (J_{sc}), and fill factor (FF). V_{oc} is directly proportional to the offset between the highest occupied molecular orbital (HOMO) level of the donor and the lowest unoccupied molecular orbital (LUMO) level of the acceptor.[7–10] A broad absorption band and balanced hole and electron mobilities of the donor/acceptor BHJ active layers of PSCs are desirable to realize higher J_{sc} and FF.[11–13] Hence, great efforts have been devoted to design and synthesize the conjugated polymer donors with low bandgap, relatively lower HOMO energy level, and higher hole mobility for high efficiency PSCs.[14–22]

Among various conjugated polymer donor materials, polythiophene (PT) derivatives have attracted considerable interest due to their high hole mobility and simple synthesis.[23–26] As the most classical PT derivative, regioregular poly(3-hexylthiophene) (P3HT) has played a critical role in the development of PSCs. However, the optimized PSCs based on the blend of P3HT and PCBM only exhibited a PCE of ≈4%, limited by relatively low V_{oc} of ≈0.60 V which is caused by the high-lying HOMO level of P3HT.[27–29] In order to solve these issues, one successful method is to raise the LUMO energy level of the acceptors for high V_{oc}.[30,31] For example, the indene bisadduct fullerene derivatives such as indene-C_{70}-bisadduct ($IC_{70}BA$) synthesized by He et al.[30b] exhibited a higher LUMO of −3.71 eV compared with that of [6,6]-phenyl-C_{61}-butyric acid methyl ester ($PC_{61}BM$) or [6,6]-phenyl-C_{71}-butyric acid methyl ester ($PC_{71}BM$) (−3.90 eV), then the PSCs based on P3HT:$IC_{70}BA$ shows the improved PCE of ≈7.4% with increased V_{oc} of 0.87 V compared to the PSCs based on P3HT:$PC_{71}BM$ (PCE of ≈4.4% and V_{oc} of 0.61 V).[23] Another strategy is to design and synthesize new PT derivatives with deep HOMO energy level by modification of side chains.[3,25,32,33] For instance, Zhang et. al. synthesized a PT derivative, PDCBT, by attaching electron-withdrawing carboxylate substituents on PT backbone, and the HOMO level of PDCBT (−5.26 eV) decreased by 0.36 eV in comparison with P3HT (−4.90 eV).[25] As a result, the corresponding PSCs showed an enhanced PCE of 7.2% with increased V_{oc} of 0.91 V. In addition, to construct the D-A type PT derivatives by introducing the thiophene-based acceptor units has been proved to be an effective way to modulate the energy levels of PT derivatives.[24,34] The PT derivative PBT1 with the thiophene fused benzodithiophene-4,8-dione (BDD) acceptor unit was reported and showed a lower HOMO level (−5.13 eV), and an improved PCE of 6.88% was achieved with V_{oc} of 0.83 V in the PBT1-based PSCs.[24] More interestingly, this method can simultaneously reduce the bandgap of PT derivatives, resulting in the broadening of absorption, which benefits for increasing J_{sc} and PCE. Therefore, the performance of PSCs based on the PT derivatives with D-A structure still has great room for improvement.

Recently, fluorination has attracted much attention due to its multiple effects on the photophysical properties of conjugated polymers, i.e., the strong electron-withdrawing ability of fluorine atom can effectively modulate the energy levels of polymers with minor effect on their bandgaps and induce the strong dipole along C—F bond, resulting in the strong inter/intramolecular interaction which benefits the excitons dissociation and charge carries transport.[35–45] Hence, in this work, we designed and synthesized a novel D-A structured PT derivative, PBDD-ff4T, based on BDD as acceptor unit and difluorinated bithiophene (ff2T) as donor unit. By introducing two strong electron-withdrawing fluorine atoms to the bithiophene unit in the polymer backbone, PBDD-ff4T showed lower HOMO level of −5.42 eV, smaller optical bandgap (E_g^{opt}) of 1.74 eV, and a higher crystallinity compared to the analog polymer PBT1 without fluorine substituent (HOMO = −5.13 eV and E_g^{opt} = 1.77 eV).[24] The lower HOMO level and smaller bandgap could be beneficial for improving the V_{oc} and J_{sc} in PSCs. As a result, the PBDD-ff4T/$PC_{71}BM$-based PSCs under optimal conditions exhibit the highest PCE of 9.2% with V_{oc} of 0.95 V, J_{sc} of 13.2 mA cm^{-2}, and FF of 73%. This value of PCE is one of the highest values reported in the literature so far for the PSCs

Q. Fan, W. Su, Prof. X. Guo, B. Guo, W. Li, Dr. Y. Zhang, Dr. K. Wang, Prof. M. Zhang, Prof. Y. Li
Laboratory of Advanced Optoelectronic Materials
College of Chemistry
Chemical Engineering and Materials Science
Soochow University
Suzhou 215123, China
E-mail: guoxia@suda.edu.cn; mjzhang@suda.edu.cn; liyongfang@suda.edu.cn, liyf@iccas.ac.cn
Prof. Y. Li
Beijing National Laboratory for Molecular Sciences
CAS Key Laboratory of Organic Solids
Institute of Chemistry
Chinese Academy of Sciences
Beijing 100190, China

DOI: 10.1002/aenm.201600430

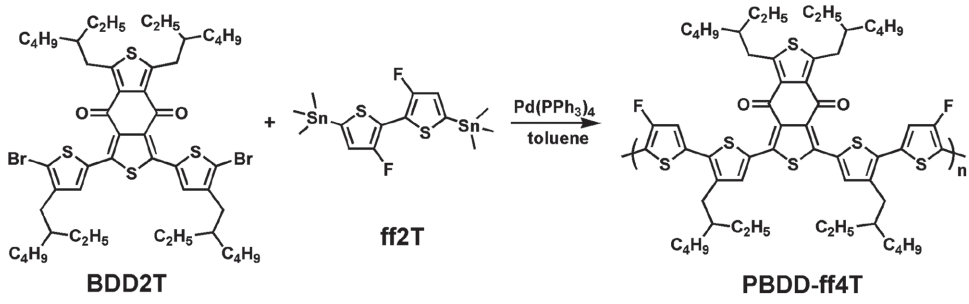

Scheme 1. Synthetic route and molecular structure of PBDD-ff4T.

based on PT derivatives. Furthermore, the performance of the PSCs based on PBDD-ff4T/$PC_{71}BM$ is insensitive to variations of active layer thickness in the range of 70–250 nm, which will be beneficial for the large scale manufacturing of high efficiency PSCs.

PBDD-ff4T was synthesized by palladium catalyzed Stille polymerization between BDD2T and ff2T, as shown in **Scheme 1**, with a yield of 71%. The number-average molecular weight (M_n) and polydispersity index (PDI) of the polymer are 13.3 kDa and 1.84, respectively. It should be mentioned that the molecular weight of 13.3 kDa was obtained by high temperature gel permeation chromatography (GPC) using monodispersed polystyrene as the standard and 1,2,4-trichlorobenzene as the eluent at 160 °C, which is smaller but more accurate than those measured by low temperature GPC with chloroform as eluent. Actually, the M_n of PBDD-ff4T measured by low temperature GPC using chloroform as the eluent was 56.9 kDa (due to the sample aggregation in the measurement) with a PDI of 1.41. The M_n of 56.9 kDa is 1.5 times of that (M_n = 38 kDa, PDI = 2.12) of the analog polymer PBT1 measured under the same measurement condition.[24] The polymer exhibits excellent solubility in common organic solvents, such as chloroform, chlorobenzene, and *o*-dichlorobenzene.

In the thermogravimetric analysis, the polymer exhibits a decomposition temperature of 429 °C with 5% weight-loss (see Figure S1 in the Supporting Information) under inert atmosphere, which indicates a good thermal stability for PSCs application. We also performed the differential scanning calorimetry (DSC) analysis for investigating the crystallinity of PBDD-ff4T, as shown in **Figure 1**a. PBDD-ff4T showed a higher melting temperature (T_m) at 235.0 °C and a higher crystallization temperature (T_c) at 223.5 °C, in comparison with a T_m of 228.3 °C and a T_c of 206.3 °C for the analog polymer PBT1 without fluorine substitution.[24] Furthermore, the crystallization enthalpy of PBDD-ff4T was found to be 14.7 J g^{-1}, which is higher than that (13.5 J g^{-1}) of the analog polymer PBT1 and regioregular P3HT.[24] The higher T_m and T_c temperatures and higher crystallization enthalpy imply that PBDD-ff4T has a stronger intermolecular interaction due to the introduction of its fluorine substitution.

In order to further study the crystallinity of the polymer, we carried out X-ray diffraction (XRD) analysis for PBDD-ff4T film, as shown in Figure 1b. A clear and intense (100) diffraction peak at $2\theta = 5.2°$ is observed in the pure PBDD-ff4T film. Notably, PBDD-ff4T film has the additional (200) diffraction peak at $2\theta = 10.4°$ and (300) diffraction peak at $2\theta = 15.6°$ compared to PBT1,[24] which implies that the polymer PBDD-ff4T has a better crystallinity, and this result is consistent with the DSC result mentioned above.

Figure 2a shows UV–vis absorption spectra of PBDD-ff4T in $CHCl_3$ solution and solid film. The absorption spectrum of the polymer in solution showed a maximum absorption (λ_{max}) at 525 nm. Notably, PBDD-ff4T shows a redshift of absorption compared to the analog polymer PBT1,[24] which can be attributed to the strong aggregation phenomenon of PBDD-ff4T in solution. In the solid film, the absorption peak is redshifted to 592 nm and an enhanced absorption shoulder peak at 639 nm can be observed, due to the strong intermolecular π–π stacking interaction of the polymer.[25] The absorption

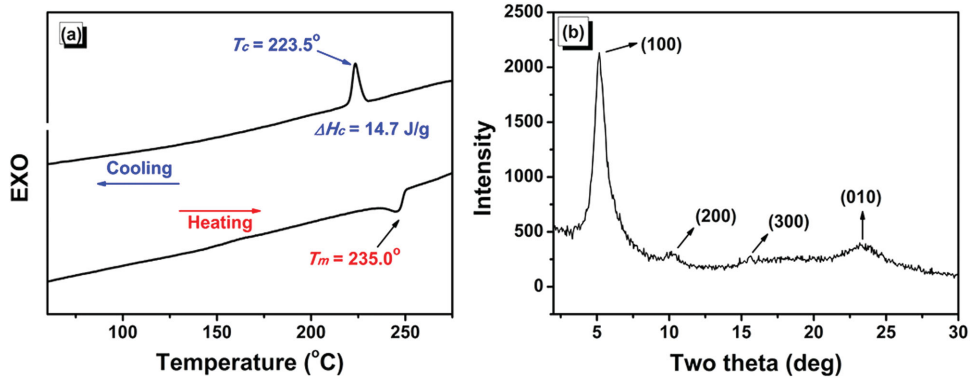

Figure 1. a) DSC plot of PBDD-ff4T with a scan rate of 2 °C min^{-1} under nitrogen atmosphere. b) XRD pattern of the pure PBDD-ff4T film.

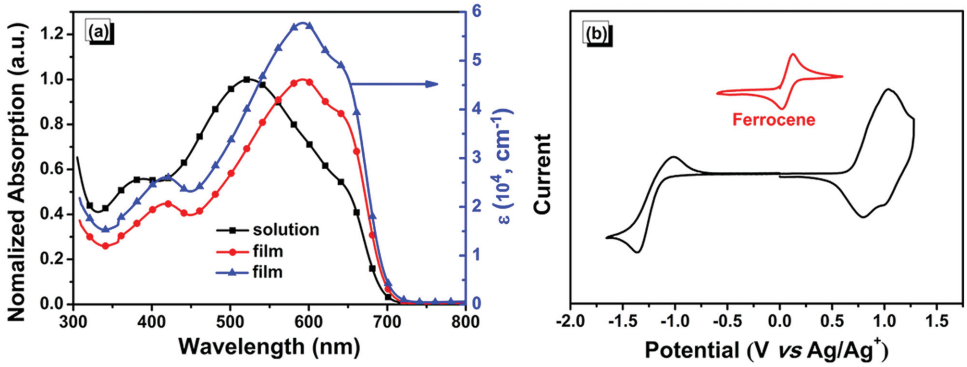

Figure 2. a) UV–vis absorption spectra of PBDD-ff4T in $CHCl_3$ solution and film; b) Cyclic voltammogram of PBDD-ff4T film on a glassy carbon electrode measured in a 0.1 mol L^{-1} Bu_4NPF_6 acetonitrile solution at a scan rate of 50 mV s^{-1}.

edge (λ_{onset}) of PBDD-ff4T is located at 714 nm corresponding to the bandgap (E_g^{opt}) of 1.74 eV in its thin film. Furthermore, compared to the analog polymer PBT1 without fluorine substituent (λ_{max} = 588 nm and E_g^{opt} = 1.77 eV),[24] PBDD-ff4T shows redshift of the absorption peak and the absorption edge due to the introduced inter and/or intramolecular F—H hydrogen bond effect and the induced dipole along C—F bond to facilitate better π–π stacking and greater extent of backbone ordering.[39,40] The less redshift of the PBDD-ff4T film than its solution, in comparison with PBT1, should be ascribed to the existence of strong aggregation of PBDD-ff4T molecules in its solution due to its fluorine substitution. Meanwhile, PBDD-ff4T showed a high hole mobility of 2.61×10^{-3} cm^2 V^{-1} s^{-1} measured by the space charge limited current method (Figure S2, Supporting Information).

The HOMO and LUMO energy levels of PBDD-ff4T were measured by electrochemical cyclic voltammetry. Figure 2b shows the cyclic voltammogram of PBDD-ff4T film. The onset oxidation and reduction potentials (E_{ox}/E_{red}) of PBDD-ff4T are 0.71 and −1.18 V versus Ag/Ag^+, and the corresponding HOMO/LUMO levels are estimated to be −5.42 and −3.53 eV according to the empirical equations:[10] HOMO = $-e(E_{ox} + 4.71)$ eV and LUMO = $-e(E_{ox} + 4.71)$ eV, respectively. Obviously, compared to PBT1 without fluorine substituent (HOMO of −5.13 eV),[24] PBDD-ff4T possesses a lower HOMO level (decreased by 0.29 eV) due to the strong electron-withdrawing ability of fluorine substituents, which is beneficial for achieving higher V_{oc} in PSCs.

The photoluminescence (PL) spectra of the pure polymer PBDD-ff4T, PBT1, and their blend films with $PC_{71}BM$ were measured with excited light at 580 nm, for investigating the photoinduced electron transfer behavior between the polymer donors and the $PC_{71}BM$ acceptor. As shown in Figure S3 of the Supporting Information, the blend film of PBDD-ff4T/$PC_{71}BM$ demonstrated 96% PL quenching of PBDD-ff4T in comparison with the PL spectrum of pure PBDD-ff4, which is higher than that (81.3% PL quenching) of the PBT1/$PC_{71}BM$ blend film. The results indicate that there is more effective photoinduced charge transfer between PBDD-ff4T and $PC_{71}BM$ than that between PBT1 and $PC_{71}BM$, and PBDD-ff4T is a suitable polymer donor matching with the $PC_{71}BM$ acceptor for the application in PSCs.

To investigate the photovoltaic properties of PBDD-ff4T, the PSCs were fabricated with a conventional device architecture of ITO/PEDOT:PSS/PBDD-ff4T:$PC_{71}BM$/PrC60MAIodide Salt(or Ca)/Al (see Figure S4 in the Supporting Information), and were characterized under the illumination of AM 1.5G (100 mW cm^{-2}). **Table 1** lists the photovoltaic performance data of the PSCs with different fabrication conditions for a clear comparison. First, the donor/acceptor (D/A, PBDD-ff4T/$PC_{71}BM$) weight ratios (w/w) in the active layer were optimized in the range of D/A ratios from 1.5:1, 1:1 to 1:1.5 for the PSCs with PrC60MAIodide Salt/Al as cathode. **Figure 3**a shows the current density–voltage (J–V) curves of devices, and we can see that all the PSCs with different D/A weight ratios in the active layer with a thickness of ≈100 nm show good photovoltaic performance with PCE higher than 8%. The optimum D/A weight ratio was found to be 1:1, the corresponding PSCs with an active layer thickness of 110 nm displayed the highest PCE of 9.2% with a V_{oc} of 0.95 V, a J_{sc} of 13.2 mA cm^{-2}, and a FF of 73%. Note that the high efficiency of 9.2% is achieved for PSCs without the thermal annealing and solvent additive treatment, which is approximately two times that of the devices based on PBT1 under the same experimental conditions without any postprocessing.[24] Furthermore, the 9.2% PCE value is ≈30% higher than that (6.88%) of the PBT1-based optimized device.[24]

The external quantum efficiency (EQE) plots of the PSCs based on PBDD-ff4T/$PC_{71}BM$ with different D/A weight ratios are shown in Figure 3b. All devices show broad EQE response in the wavelength range from ≈300 to 700 nm. The maximum EQE value was close to 73% for the champion device (1/1, w/w), indicating more efficient photon harvesting and charge collection within the cell in agreement with the PL quenching results mentioned above. According to the EQE curve and the solar irradiation spectrum, the mismatches between the integral J_{sc} values and the measured J_{sc} values are below 5%.

In the following, we used the optimized D/A weight ratio of 1:1 and carried out the investigations to study the relationship between the photovoltaic performance of the PSCs based on PBDD-ff4T/$PC_{71}BM$ (1:1, w/w) with other different fabrication conditions including active layer thickness, thermal annealing, solvent additive treatment, and the

Table 1. Photovoltaic performances of the PSCs based on PBDD-ff4T/$PC_{71}BM$ under the illumination of AM 1.5G, 100 mW cm^{-2}. Standard deviations of parameters based on ten devices are shown in parentheses.

D/A [w/w]	Thickness [nm]	V_{oc} [V]	J_{sc} [mA cm^{-2}]	FF	PCE_{ave}[h)] [%]	PCE_{max} [%]
1.5:1	130	0.97 (±0.001)	12.7 (±0.3)	0.68 (±0.02)	8.1 (±0.1)	8.3
1:1	70	0.95 (±0.001)	10.8 (±0.4)	0.72 (±0.02)	7.1 (±0.2)	7.3
1:1	95	0.96 (±0.001)	11.7 (±0.4)	0.73 (±0.01)	8.0 (±0.1)	8.2
1:1	110	0.95 (±0.001)	13.2 (±0.4)	0.73 (±0.02)	8.8 (±0.3)	9.2
1:1[a)]	110	0.95 (±0.001)	12.5 (±0.3)	0.71 (±0.01)	8.1 (±0.1)	8.3
1:1[b)]	110	0.95 (±0.001)	12.4 (±0.3)	0.71 (±0.02)	8.0 (±0.1)	8.3
1:1[c)]	110	0.95 (±0.001)	12.2 (±0.4)	0.70 (±0.02)	7.9 (±0.2)	8.1
1:1[d)]	110	0.94 (±0.001)	12.6 (±0.3)	0.72 (±0.01)	8.3 (±0.1)	8.5
1:1[e)]	110	0.93 (±0.001)	12.8 (±0.3)	0.71 (±0.02)	8.2 (±0.1)	8.3
1:1[f)]	110	0.93 (±0.001)	12.3 (±0.2)	0.71 (±0.02)	8.0 (±0.1)	8.1
1:1[g)]	110	0.88 (±0.001)	12.7 (±0.2)	0.59 (±0.03)	6.4 (±0.1)	6.6
1:1	150	0.95 (±0.001)	12.2 (±0.3)	0.71 (±0.01)	8.0 (±0.1)	8.3
1:1	250	0.93 (±0.001)	11.7 (±0.4)	0.68 (±0.02)	7.1 (±0.2)	7.3
1:1.5	125	0.96 (±0.001)	12.0 (±0.2)	0.73 (±0.02)	8.2 (±0.1)	8.4

[a)]With thermal annealing at 80 °C for 10 min; [b)]With thermal annealing at 100 °C for 10 min; [c)]With thermal annealing at 120 °C for 10 min; [d)]With 3% DIO; [e)]With 3% NMP; [f)]Ca/Al as the cathode layer; [g)]The flexible devices from over three devices; [h)]The average PCE was obtained from over ten devices.

commonly used Ca/Al cathode. **Figure 4** shows the photovoltaic performance of the PSCs with difference active layer thickness and with or without the extra treatments of thermal annealing and solvent additive, and the photovoltaic performance data are also listed in Table 1. It can be seen that the photovoltaic performance of the PSCs was not so sensitive to the active layer thickness. Even with 70 nm thickness of the active layer, PCE of the PSC still reached 7.3% with a higher J_{sc} of 10.8 mA cm^{-2}. When the thickness of the active layer gradually increased from 70 to 250 nm, the PCE values of the devices were first increasing from 7.3% for the PSC with thickness of 70 nm to 9.2% for the PSC with thickness of 110 nm, then decreasing to 7.3% for the PSC with thickness of 250 nm with the variation of (8.3 ± 0.9)%. In other words, whether the active layer is very thin (≈70 nm) or very thick (≈250 nm), the device showed the PCE value of more than 7.3% due to the virtually unchanged V_{oc} (≈0.94 ± 0.01 V) and the less changed J_{sc} (≈11.9 ± 1.3 mA cm^{-2}) values of the devices, while the FF values dropped slightly from 73% for the best device to 68% for the device with a thick active layer of 250 nm. Based on the above results, it can be concluded that the photovoltaic performance of the PSCs based on PBDD-ff4T/$PC_{71}BM$ is insensitive to the variation of active layer thickness in the range of 70–250 nm.

For studying the effect of thermal annealing treatment on the photovoltaic performance, we performed the experiments without or with the thermal annealing at 80, 100, and 120 °C, respectively, for 10 min. The PSCs with different thermal annealing temperature exhibit similar photovoltaic performance with PCE values in the range of 8.1%–8.3%, as also shown in Figure 4a and Table 1. However the PCE of the PSCs with thermal annealing was decreased in comparison with that of 9.2% for the PSCs without the thermal treatment. The results indicate that the thermal annealing is not needed for the PSCs based on PBDD-ff4T/$PC_{71}BM$, which is a significant advantage for future fabrication of flexible PSCs.

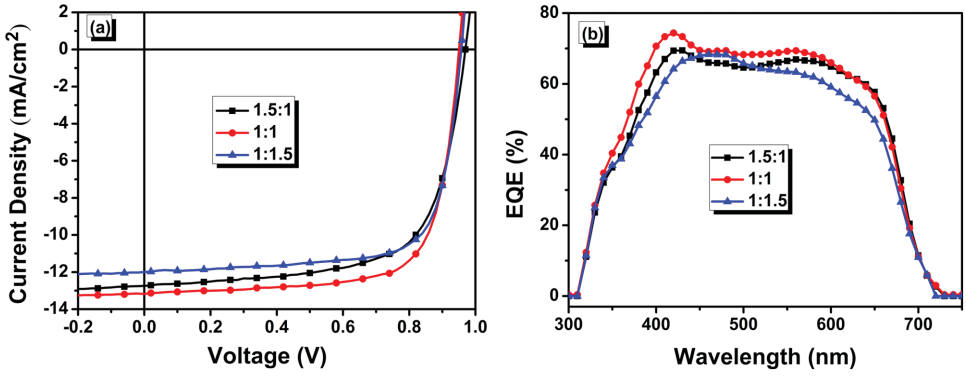

Figure 3. a) The *J–V* curves and b) EQE curves of the PSCs based on PBDD-ff4T/$PC_{71}BM$ with different D/A weight ratios.

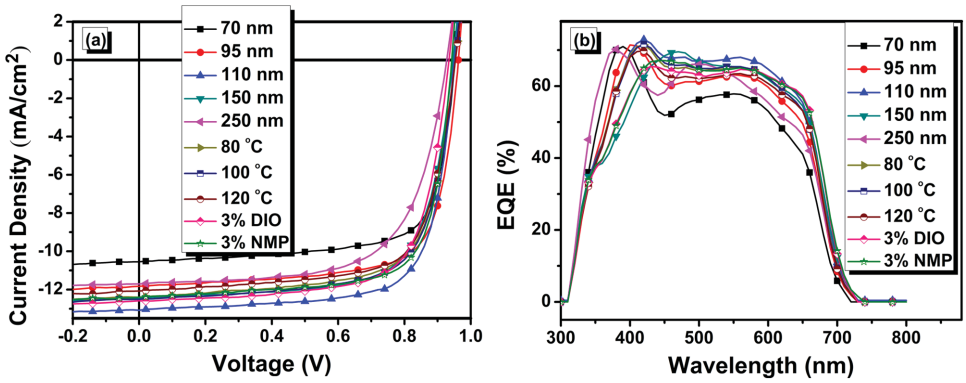

Figure 4. a) The *J–V* curves and b) EQE curves of the PSCs based on PBDD-ff4T/$PC_{71}BM$ (1:1, w/w) with different active layer thickness and with or without extra treatments of thermal annealing and solvent additive.

For investigating the effect of solvent additive on the photovoltaic performance, we used 3% (v/v) 1,8-diiodooctane (DIO) or *N*-methyl-2-pyrrolidone (NMP) as the solvent additives during fabricating the PSCs based on PBDD-ff4T/$PC_{71}BM$ (1:1, w/w). The PCE of the PSCs with the treatment of solvent additive was ≈8.3%–8.5% (Figure 4a and Table 1), which is slightly decreased in comparison with the PCE of 9.2% for the optimized PSC without the solvent additive treatment. The results indicate that the solvent additive treatment is also not needed for the PSCs based on PBDD-ff4T/$PC_{71}BM$, which is also an advantage for the large area fabrication of the PSCs in future.

We also fabricated the PSCs based on PBDD-ff4T/$PC_{71}BM$ (1:1, w/w) with Ca/Al as the cathode for comparison with the PrC60MAIodide Salt/Al cathode used in the studies of the photovoltaic performance mentioned above. The *J–V* curves and the EQE plots of the PSCs with Ca/Al cathode were shown in Figure S6 of the Supporting Information, and their photovoltaic performance data are also listed in Table 1. The PSC based on PBDD-ff4T/$PC_{71}BM$ (1:1, w/w) with Ca/Al cathode showed a PCE of 8.1% with a V_{oc} of 0.93 V, a J_{sc} of 12.2 mA cm^{-2}, and a FF of 71%, which is lower than that (PCE of 9.2%) of the device with the PrC60MAIodide Salt/Al cathode. The results indicate that PrC60MAIodide is an effective cathode buffer layer material for high performance PSCs. Notably, the PCE of 8.1% is significantly higher than that (6.88%) of the PSCs based on the analog polymer PBT1 with the same Ca/Al cathode.[24]

Stability is another important issue for the studies of PSCs. Therefore, we also investigated the photovoltaic performance degradation of the device with time prolonging (see Figure S6 in the Supporting Information). With the device storage time prolonging from 0 to 150 h in the drybox, their V_{oc} values were not changed, while the J_{sc} values were slightly reduced from 13.2 to 13.0 mA cm^{-1} and FF was also slightly decreased from 73% to 69%, resulting in a slightly reduced PCE from 9.2% to 8.5% with a small PCE loss of 7.6%. Notably, the photovoltaic performance of the PSCs remained almost unchanged from 100 to 150 h, which implies that the PSCs possess a good stability as a function of the storage time.

Finally, the flexible devices based on PBDD-ff4T/$PC_{71}BM$ (1:1, w/w) were fabricated to check the possible application of PBDD-ff4T in flexible PSCs. The detailed fabrication processes of the flexible PSCs[46] are described in the Supporting Information. The device structure of the flexible PSCs is shown in Figure S7 of the Supporting Information, and the *J–V* curve and the EQE plot of device are shown in Figure S8 of the Supporting Information. The flexible PSCs exhibit a PCE of 6.6% with V_{oc} of 0.88 V, J_{sc} of 12.8 mA cm^{-2}, and FF of 59% after our initial optimization. The PCE of 6.6% is one of the highest values reported for the polymer-based flexible devices. The above results indicate that fluorinated PBDD-ff4T is a promising photovoltaic donor material for large area manufacturing of high efficient PSCs.

To understand the surface and bulk morphologies of the blend films of PBDD-ff4T:$PC_{71}BM$, we carried out atomic force microscopy (AFM) and transmission electron microscopy (TEM) measurements. **Figure 5** shows the TEM images of PBDD-ff4T:$PC_{71}BM$ blend films without or with the solvent additive of 3% DIO or 3% NMP. The bright and dark regions in the TEM images are PBDD-ff4T-rich and $PC_{71}BM$-rich domains, respectively. The blend film without solvent additive shows a bicontinuous D/A interpenetrating network, well-developed fibrillar structure, and suitable fiber size, which would be beneficial to efficient exciton dissociation and charge transportation, and thus higher PCE value can be harvested. For the blend films with the additives treatment of DIO or NMP, the relatively obvious cluster and less-defined phase separation were observed, which are consistent with the poorer devices performance of the blend films with the treatment of solvent additive mentioned above. The AFM images of the PBDD-ff4T:$PC_{71}BM$ blend films without or with solvent additive treatment, as shown in Figure S9 of the Supporting Information, confirm the results of the TEM measurements. The root-mean-square (RMS) values are 0.81, 4.52, and 3.34 nm for the blend films processed without additive, with 3% DIO, and with 3% NMP, respectively. The larger RMS for the blend films with the treatment of additives indicates too big aggregation size of PBDD-ff4T by the additive treatment, which decreased the photovoltaic performance. In addition, the RMS value of 4.52% for the PBDD-ff4T/$PC_{71}BM$ blend film processed by DIO additive is higher than that (2.92 nm) of the PBT1/$PC_{71}BM$ blend film with the DIO additive treatment,[24] which further confirms the stronger crystallinity of PBDD-ff4T with the fluorine substitution. The results are consistent with the DSC and XRD measurements (see Figure 1).

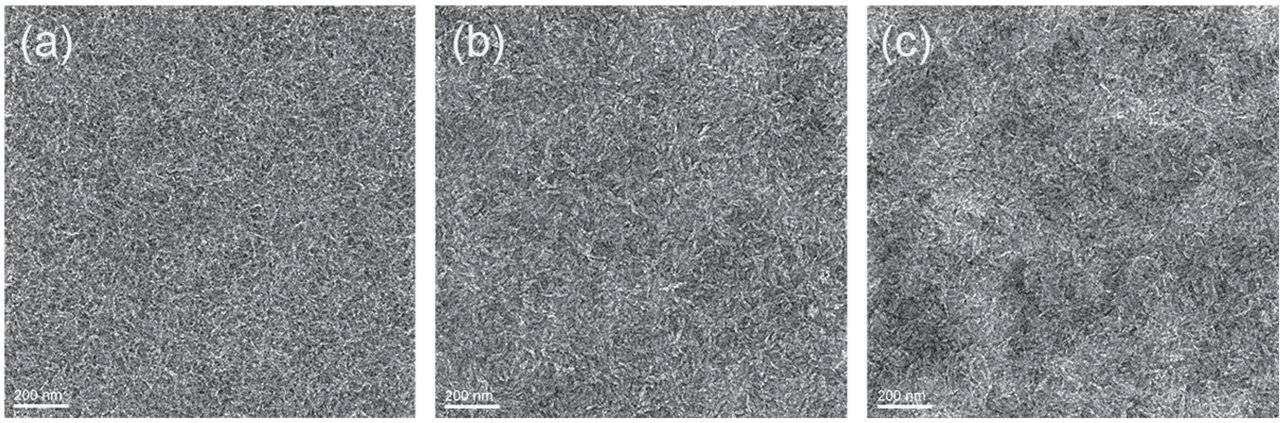

Figure 5. TEM images of PBDD-ff4T:$PC_{71}BM$ blend films: a) without additive; b) with 3% DIO; c) with 3% NMP.

In conclusion, a novel D-A structured PT derivative of PBDD-ff4T with fluorine substituent was synthesized and developed for photovoltaic applications. Compared to the analog polymer PBT1 without fluorine substituent, PBDD-ff4T exhibited a smaller bandgap, a deeper HOMO energy level, and a higher crystallinity. The PSCs based on PBDD-ff4T/$PC_{71}BM$ without any extra treatment yielded a higher PCE of 9.2% with a high V_{oc} of 0.95 V and a high FF of 73%. The PCE of 9.2% is one of the highest values reported for the PT derivatives-based PSCs. Furthermore, the photovoltaic performance of the device is insensitive to the variations of actively layer thickness and without the need of thermal annealing and solvent additive treatment, which indicate that fluorinated PBDD-ff4T is a promising candidate for the large scale manufacturing and practical application of highly efficient PSCs.

Experimental Section

Measurements and fabrication of polymer solar cells are described in the Supporting Information.

Materials: All chemicals and solvents were reagent grades and purchased from Aldrich, Alfa Aesar, and TCI. 3-Fluoro-2-(3-fluoro-5-(trimethylstannyl)thiophen-2-yl)-5-(trimethylstannyl)thiophene (ff2T) was purchased from Suna Tech Inc. 1,3-Bis(5-bromo-4-(2-ethylhexyl)-thiophen-2-yl)-5,7-bis(2-ethylhexyl)benzo[1,2-*c*:4,5-*c*′]dithiophene-4,8-dione (BDD2T) was synthesized according to procedure reported in the literature.[24]

Synthesis of PBDD-ff4T: Polymer PBDD-ff4T was synthesized from BDD2T and ff2T according to Scheme 1. In a dry 50 mL flask, tetrakis(triphenylphosphine)palladium (15.0 mg) was added to a solution of BDD2T (192 mg, 0.2 mmol) and ff2T (106 mg, 0.2 mmol) in 10 mL degassed toluene under nitrogen and stirred vigorously at 110 °C for 24 h. Then the mixture was poured into methanol (80 mL) and the precipitation was occurred. The polymer was dissolved in chloroform and the solution was filtered through a silica gel column. The collected chloroform solution was concentrated and precipitated with methanol to get the dark solid (146 mg, 71%). ^{1}H NMR (400 MHz, $CDCl_3$, TMS), δ (ppm): 7.58–7.55 (br, 2H), 7.02–6.97 (br, 2H), 3.31–3.29 (br, 4H), 2.74–2.72 (br, 4H), 1.76–1.71 (br, 4H), 1.30–1.28 (br, 32H), 0.99–0.86 (br, 24H). Anal. Calcd for $C_{58}H_{74}F_2N_2O_2S_6$ (%): C, 67.40; H, 7.22. Found (%): C, 67.11; H, 7.49.

Supporting Information

Supporting Information is available from the Wiley Online Library or from the author.

Acknowledgements

Q.F. and W.S. contributed equally to this work. This work was supported by National Natural Science Foundation of China (NSFC) (Grant Nos. 91333204, 51203168, 51422306, 51503135, and 51573120), the Priority Academic Program Development of Jiangsu Higher Education Institutions, Jiangsu Provincial Natural Science Foundation (Grant No. BK20150332), Natural Science Foundation of the Jiangsu Higher Education Institutions of China (Grant No. 15KJB430027), and the Ministry of Science and Technology of China (973 project, No. 2014CB643501).

Received: February 26, 2016
Revised: April 9, 2016
Published online: May 17, 2016

[1] Y. F. Li, *Acc. Chem. Res.* **2012**, *45*, 723.
[2] L. Lu, M. A. Kelly, W. You, L. P. Yu, *Nat. Photonics* **2015**, *9*, 491.
[3] Z. G. Zhang, Y. F. Li, *Sci. China Chem.* **2015**, *58*, 192.
[4] E. G. Wang, W. Mammo, M. R. Andersson, *Adv. Mater.* **2014**, *26*, 1801.
[5] K. R. Graham, C. Cabanetos, J. P. Jahnke, M. N. Idso, A. Amassian, P. M. Beaujuge, M. D. McGehee, *J. Am. Chem. Soc.* **2014**, *136*, 9608.
[6] J. S. Wu, S. W. Cheng, Y. J. Cheng, C. S. Hsu, *Chem. Soc. Rev.* **2015**, *44*, 1113.
[7] P. W. M. Blom, V. D. Mihailetchi, L. J. A. Koster, D. E. Markov, *Adv. Mater.* **2007**, *19*, 1551.
[8] a) M. J. Zhang, X. Guo, W. Ma, H. Ade, J. H. Hou, *Adv. Mater.* **2015**, *27*, 4655; b) S. Q. Zhang, L. Ye, W. C. Zhao, B. Yang, Q. Wang, J. H. Hou, *Sci. China Chem.* **2015**, *58*, 248.
[9] a) Q. P. Fan, M. Xiao, Y. Liu, W. Y. Su, H. Gao, H. Tan, Y. Wang, G. Lei, R. Yang, W. G. Zhu, *Polym. Chem.* **2015**, *6*, 4290; b) Q. P. Fan, H. Jiang, Y. Liu, W. Y. Su, H. Tan, Y. Wang, R. Yang, W. G. Zhu, *J. Mater. Chem. C* **2016**, *4*, 2606.
[10] a) J. H. Hou, Z. Tan, Y. Yan, Y. He, C. Yang, Y. F. Li, *J. Am. Chem. Soc.* **2006**, *128*, 4911; b) M. J. Zhang, X. Guo, S. Zhang, J. H. Hou, *Adv. Mater.* **2014**, *26*, 1118.

[11] Y. Xu, C. Chueh, H. Yip, F. Ding, Y. Li, C. Li, X. Li, W. Chen, A. K. Jen, *Adv. Mater.* **2012**, *24*, 6356.
[12] a) Q. P. Fan, Y. Liu, M. Xiao, W. Y. Su, H. Gao, J. Chen, H. Tan, Y. Wang, R. Yang, W. G. Zhu, *J. Mater. Chem. C* **2015**, *3*, 6240; b) Q. P. Fan, X. Xu, Y. Liu, W. Y. Su, X. He, Y. Zhang, H. Tan, Y. Wang, Q. Peng, W. G. Zhu, *Polym. Chem.* **2016**, *7*, 1747.
[13] L. J. Huo, T. Liu, X. Sun, Y. Cai, A. J. Heeger, Y. M. Sun, *Adv. Mater.* **2015**, *27*, 2938.
[14] a) C. H. Cui, W. Y. Wong, Y. F. Li, *Energy Environ. Sci.* **2014**, *7*, 2276; b) C. H. Cui, Z. C. He, Y. Wu, X. Cheng, H. B. Wu, Y. F. Li, Y. Cao, W.-Y. Wong, *Energy Environ. Sci.* **2016**, *9*, 885.
[15] a) Y. Liu, J. Zhao, Z. Li, C. Mu, W. Ma, H. Hu, K. Jiang, H. Lin, H. Ade, H. Yan, *Nat. Commun.* **2014**, *5*, 6293. b) Y. F. Li, *Sci. China Chem.* **2015**, *58*, 188.
[16] M. J. Zhang, X. Guo, W. Ma, S. Zhang, L. J. Huo, H. Ade, J. H. Hou, *Adv. Mater.* **2014**, *26*, 2089.
[17] M. Wang, H. Wang, T. Yokoyama, X. Liu, Y. Huang, Y. Zhang, T. Nguyen, S. Aramaki, G. C. Bazan, *J. Am. Chem. Soc.* **2014**, *136*, 12576.
[18] X. Guo, M. J. Zhang, J. H. Tan, S. Q. Zhang, L. J. Huo, W. P. Hu, Y. F. Li, J. H. Hou, *Adv. Mater.* **2012**, *24*, 6536.
[19] Z. Chen, P. Cai, J. Chen, X. Liu, L. Zhang, L. Lan, J. Peng, Y. Ma, Y. Cao, *Adv. Mater.* **2014**, *26*, 2586.
[20] C. Cabanetos, A. E. Labban, J. A. Bartelt, J. D. Douglas, W. R. Mateker, M. D. McGehee, P. M. Beaujuge, *J. Am. Chem. Soc.* **2013**, *135*, 4656.
[21] J. W. Jo, J. W. Jung, E. H. Jung, H. Ahn, T. J. Shin, W. H. Jo, *Energy Environ. Sci.* **2015**, *8*, 2427.
[22] Y. Deng, J. Liu, J. Wang, L. Liu, W. Li, H. Tian, X. Zhang, Z. Xie, Y. Gen, F. Wang, *Adv. Mater.* **2014**, *26*, 471.
[23] X. Guo, C. H. Cui, M. J. Zhang, L. J. Huo, Y. Huang, J. H. Hou, Y. F. Li, *Energy Environ. Sci.* **2012**, *5*, 7943.
[24] D. Qian, W. Ma, Z. Li, X. Guo, S. Zhang, L. Ye, H. Ade, Z. Tan, J. H. Hou, *J. Am. Chem. Soc.* **2013**, *135*, 8464.
[25] M. J. Zhang, X. Guo, W. Ma, H. Ade, J. H. Hou, *Adv. Mater.* **2014**, *26*, 5880.
[26] Z. G. Zhang, S. Zhang, J. Min, C. H. Chui, J. Zhang, M. J. Zhang, Y. F. Li, *Macromolecules* **2012**, *45*, 113.
[27] W. Ma, C. Yang, X. Gong, K. Lee, A. J. Heeger, *Adv. Funct. Mater.* **2005**, *15*, 1617.
[28] G. Li, V. Shrotriya, J. Huang, Y. Yao, T. Moriarty, K. Emery, Y. Yang, *Nat. Mater.* **2005**, *4*, 864.
[29] M. T. Dang, L. Hirsch, G. Wantz, J. D. Wuest, *Chem. Rev.* **2013**, *113*, 3734.
[30] a) Y. J. He, H. Chen, J. H. Hou, Y. F. Li, *J. Am. Chem. Soc.* **2010**, *132*, 1377. b) Y. He, G. Zhao, B. Peng, Y. F. Li, *Adv. Funct. Mater.*, **2010**. *20*: 3383.
[31] G. J. Zhao, Y. J. He, Y. F. Li, *Adv. Mater.* **2010**, *22*, 4355.
[32] J. H. Hou, T. L. Chen, S. Zhang, L. Huo, S. Sista, Y. Yang, *Macromolecules* **2009**, *42*, 9217.
[33] M. J. Zhang, X. Guo, Y. Yang, J. Zhang, Z. G. Zhang, Y. F. Li, *Polym. Chem.* **2011**, *2*, 2900.
[34] J. Kim, J. B. Park, I. H. Jung, A. C. Grimsdale, S. C. Yoon, H. Yang, D. Hwang, *Energy Environ. Sci.* **2015**, *8*, 2352.
[35] a) H. Zhou, L. Yang, A. C. Stuart, S. C. Price, S. Liu, W. You, *Angew. Chem. Int. Ed.* **2011**, *50*, 2995; b) W. Li, S. Albrecht, L. Yang, S. Roland, J. R. Tumbleston, T. McAfee, L. Yan, M. A. Kelly, H. Ade, D. Neher, W. You, *J. Am. Chem. Soc.* **2014**, *136*, 15566.
[36] D. Dang, W. Chen, S. Himmelberger, Q. Tao, A. Lundin, R. Yang, W. Zhu, A. Salleo, C. Müller, E. Wang, *Adv. Energy Mater.* **2014**, *4*, 1400680.
[37] a) Q. P. Fan, Y. Liu, P. Yang, W. Y. Su, M. Xiao, J. Chen, M. Li, X. Wang, Y. Wang, H. Tan, R. Yang, W. G. Zhu, *Org. Electron.* **2015**, *23*, 124; b) Q. P. Fan, Y. Liu, H. Jiang, W. Su, L. Duan, H. Tan, Y. Li, J. Deng, R. Yang, W. G. Zhu, *Org. Electron.* **2016**, *33*, 128.
[38] P. Liu, K. Zhang, F. Liu, Y. Jin, S. Liu, T. P. Russell, H. Yip, F. Huang, Y. Cao, *Chem. Mater.* **2014**, *26*, 3009.
[39] T. L. Nguyen, H. Choi, M. A. Uddin, B. Walker, S. Yum, M. H. Yun, T. J. Shin, S. Hwang, J. Y. Kim, H. Y. Woo, *Energy Environ. Sci.* **2014**, *7*, 3040.
[40] J. Jheng, Y. Lai, J. Wu, Y. Chao, C. Wang, C. Hsu, *Adv. Mater.* **2013**, *25*, 2445.
[41] J. W. Jung, F. Liu, T. P. Russell, W. H. Jo, *Adv. Energy Mater.* **2015**, *5*, 1500065.
[42] D. Liu, W. Zhao, S. Zhang, L. Ye, Z. Zheng, Y. Cui, Y. Chen, J. H. Hou, *Macromolecules* **2015**, *48*, 5172.
[43] J.-H. Kim, S. A. Shin, J. B. Park, C. E. Song, W. S. Shin, H. Yang, Y. F. Li, D.-H. Hwang, *Macromolecules* **2014**, *47*, 1613.
[44] J. Min, Z.-G. Zhang, S. Zhang, Y. F. Li, *Chem. Mater.* **2012**, *24*, 3247.
[45] S. Q. Zhang, L. Ye, J. H. Hou, *Adv. Energy Mater.* **2016**, *6*, DOI: 10.1002/aenm.201502529.
[46] Y. Li, L. Meng, Y. (Michael) Yang, G. Xu, Z. Hong, Q. Chen, J. You, G. Li, Y. Yang, Y. Li, *Nat. Commun.* **2016**, *7*, 10214.

